euspen's 22nd International Conference & Exhibition, Geneva, CH, May/June 2022
www.euspen.eu

In-mould measurement with optical coherence tomography for compensating positioning error in injection overmoulding of optoelectronic devices

Günther Hannesschläger[1], Martin Schwarze[2], Elisabeth Leiss-Holzinger[1], Christian Rankl[1]

[1] *Research Center for Non-Destructive Testing GmbH (RECENDT), Linz, Austria*
[2] *Fraunhofer-Institut für Werkzeugmaschinen und Umformtechnik, Chemnitz, Germany*

guenther.hannesschlaeger@recendt.at

Abstract
In this work we present an optical coherence tomography (OCT) setup for in-mould measurements, which is combined with a mechatronic actuator, that adjusts the position of an opto-electronic part (LED), which will be overmoulded with a lens-shaped structure to form a fiber optic transceiver (FOT). In particular, the lens increases the coupling efficiency of the LED, and precise positioning with respect to the mould (lens) will increase the overall product quality. This work is part of the EU-funded project FLOIM (Flexible Optical Injection Moulding of optoelectronic devices).
The OCT measurement is applied before the overmoulding process, to find out the displacement of the LED. The calculated LED displacement is passed to the control unit of the mechatronic device, which in turn corrects the displacement by moving the sample. It is shown that the overall concept is feasible, and it is also pointed out where additional research is required.

Keywords: Optical Coherence Tomography, high-precision injection moulding, in-mould sensors, optoelectronics

1. Introduction

Micro injection moulding has become increasingly important in mass production of high precision optical parts [1]. As for every optical element, surface quality, surface precision and material homogeneity are of crucial importance.

Direct overmoulding of optoelectronic parts with optical elements offers significant advantages over conventional assembling. However, these advantages can only be used to the full, if the overmoulded structure is precisely aligned to the part it should serve. Therefore, a sensor/actuator system is needed, that is able to detect and correct the displacement between the part to be overmoulded and the mould.

An elegant approach for displacement correction with a mechatronic fixture has already been presented [2]. In this work we describe the in-mould-sensor that delivers the sensoric data for getting a complete control cycle. Since traditional in-mould sensors cannot provide sufficient displacement data [3], a novel approach using optical coherence tomography (OCT) is used.

It is shown, that the OCT sensor and the mechatronic fixture are capable of correcting the displacement with sufficient precision at high accuracy. In addition to the in-plane displacement the OCT measurement can provide information about the height of the sample and, if performed after the injection process, about inhomogeneities in the injected material, such as bubbles or cracks. This was a reason why OCT was preferred in this research project. However, this is not covered in this paper.

2. Optical coherence tomography

OCT is a non-contact, non-destructive, fast and robust measurement technology. It is capable of acquiring 3D data with micrometer resolution. In addition to medical applications in ophthalmology and dermatology [4, 5], more and more industrial applications have been established [6]. For this work so called spectral-domain-OCT (SD-OCT) has been used.

2.1. Measurement principle SD-OCT

The basic principle of OCT can be seen in figure 1. It is based on white-light interferometry, where the incoming broadband light beam is divided into a reference- and a sample beam. The light that is reflected both from the reference mirror and various positions on and inside the sample interfere with each other. In SD-OCT a spectrometer is used to detect the output of the interferometer, also called interferogram. It contains information about the inner structure of the sample. A couple of signal processing steps then provide a depth scan, or A-scan [7]. This procedure can be repeated while raster-scanning the beam over the sample to form a 3D data cube. Scanning along a straight line results in a cross-sectional-image, or B-scan.

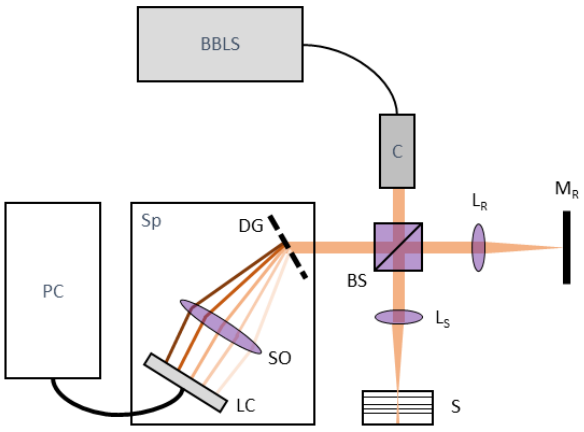

Figure 1. Principle of SD-OCT. BBLS: Broadband Lightsource, BS: Beamsplitter, L_R: Lens in reference path, M_R: Reference mirror, L_S: Lens in sample path, S: Sample, Sp: Spectrometer, DG: Diffraction grating, SO: spectrometer objective lens system, LC: Linecamera, PC: Personal computer.

Typically the probe head of an SD-OCT setup contains an interferometer, galvanometer scanning mirrors and an objective lens. Depending on the geometric boundary conditions of the particular application probe heads can have varying designs.

Other components, like the light source, the spectrometer, driver boards, power sources and the computer are placed in a separate housing.

2.2. Description of the application

Before starting to design the OCT setup, a set of specifications had to be determined, which mainly depended on the targeted samples, in this case a fiber optic transceiver (FOT). The general design of an FOT before the overmoulding step (view from top) is shown in figure 2. The leadframe helps to position the part in the mould and is cut away later. On the metal leadframe the die and the LED are mounted on top of each other. Some dimensions and other specifications are listed in table 1.

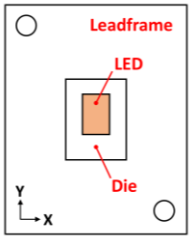

Figure 2. FOT Schematic, view from top. Leadframe with die and LED stacked on each other.

Table 1. FOT Specifications.

Specifications of FOT	
Position tolerance relative to FOT	50 µm (X and Y direction)
Fabrication tolerance	20 µm
Angular tolerance	0.06°
Refractive index of injected material	1.531
Lateral dimensions	< 1 mm squared
Height (non overmoulded)	< 500 µm
Height (overmoulded)	2.5 mm

2.3. In-mould OCT-setup

For designing the OCT setup and the in-mould probe head the following boundary conditions had to be taken into account:

Environmental conditions: A robust 19-inch-housing for industrial use was chosen to contain all components except for the probe head. Figure 3 shows the front-top view of the case, with the glass fiber and electrical cables leading to the probe head.

Sample size: A maximum scanning area of 2 mm squared was sufficient for covering the whole sample. As depth range 4.2 mm was chosen, so that changes in optical path length due to the refractive index of the injected material could be covered.

Mould design: due to the injection moulding process the mould has a fixed (lower) and a moveable (upper) part, the movement is in vertical direction. Since the OCT beam needed to illuminate the sample from above, the sample path was designed to enter the mould from the side and then make a 90 degree bend. Therefore the head design had to be split into a fixed and a moveable part. As shown in figure 4 only the passive optical elements in the sample path (lens, mirror and viewport) were built into the moveable part.

Mould dimensions and material: The cavity being located 50 mm inside the mould resulted in a minimum sample path length of 80 mm. An objective lens with 50 mm focal length was chosen. The probe head material had to match the material of the mould, to reduce errors due to thermal expansion.

Figure 3. 19″-housing for OCT components.

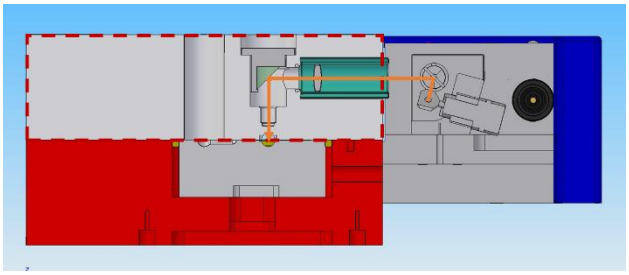

Figure 4. CAD cross sectional image of probe head and part of the mould. The red dashed line marks the vertically moveable upper part. The orange line indicates the sample beam between the galvo scanners and the cavity.

Figure 5 shows the manufactured probe head mounted on a 3D-printed dummy mould, which includes the sample path. Table 2 lists the general specifications of the designed OCT system.

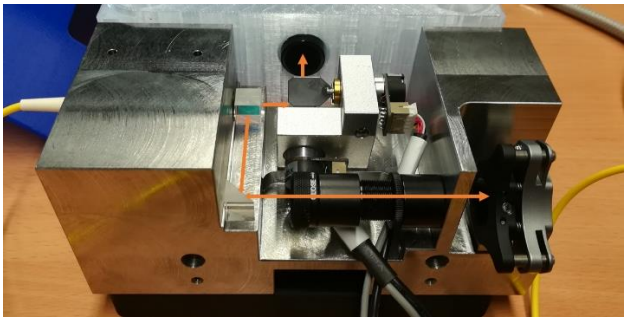

Figure 5. Probe head with dummy mould and without cover. The added orange lines mark the beam paths (reference path in the front, sample path in the back).

Table 2. OCT system specifications.

Specifications of OCT system	
Type	SD-OCT
Wavelength	840 nm
Bandwidth	65 nm
Axial resolution	5 µm
Lateral resolution	15 µm
A-scan acquisition rate	60 kHz
Volume-scan duration	< 10 s
Depth range	4.2 mm
Lateral scan range (max)	5 mm squared

3. OCT data processing

As described in section 2.1 the 3D volume data is obtained by scanning the light beam across the surface in X- and Y-direction, while acquiring A-scans (Z-direction). Figure 6 shows the corresponding coordinate system of such a 3D image stack. The red bar indicates the region of depth layers that are used to

compute a sum image. This sum image is then compared to a reference image, as shown in figure 7. Since the mechatronic fixture only corrects in-plane displacement, the image processing focuses on orthogonal lateral and angular displacement. For the former cross-correlation of reference and current image proved to give best results. For the latter a routine comprising Canny edge-detection, followed by Hough-transform and stepwise search for the angular displacement was implemented. The experiments showed that angular displacement was beyond detectability, so only the lateral displacement needed to be compensated. The processing is described in figure 7.

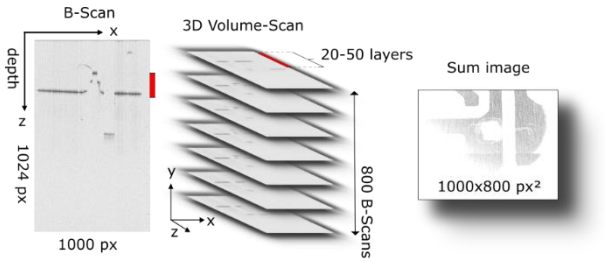

Figure 6. Coordinate system of 2D-Scan, sketched with real data B-Scans. The depth region that corresponds to the sum-image is indicated red.

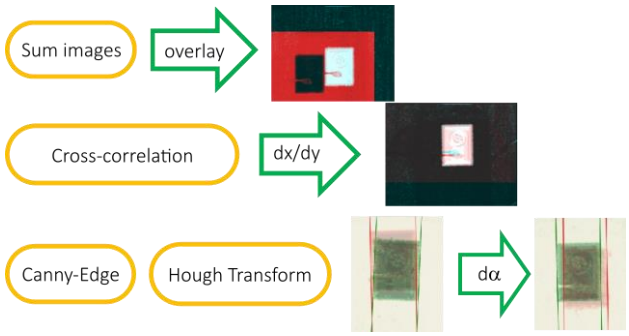

Figure 7. Processing of the OCT images to obtain displacement values.

4. In-mould measurements

The main task of this work was to combine the OCT sensor and the mechatronic fixture. So the OCT device was transported to Chemnitz, Germany, and set up in the labs of Fraunhofer IWU. Prior to these tests careful preparations have been made to allow a quick and smooth combination of the two parts. Since displacement correction required the sample to be moveable, it was decided to leave a 1 mm gap between upper and lower part of the mould.

After a tactile measurement of the compliant mechanism, it was found that the wire erosion process, even with greatly reduced process parameters, leads to shape deviations of the solid cones and in particular the parallelism of the piezo actuator receptacles in the range of up to 30 µm due to the heat input. These deviations have a significant influence on the transmission accuracy of the actuator stroke. After assembling the injection mould, the positioning accuracy of the axes was therefore first measured, the influences of the sensor and control technology were investigated and then a compensation strategy was developed.

4.1. Positioning accuracy of mechatronic fixture

A Renishaw laser interferometer measuring system with a maximum measuring accuracy of 0.1 µm was used to measure the positioning accuracy of the mechatronic axes. For this purpose, the motion control system on the NI CompactRio module and the data from the direct measuring system around the mould core was used for position control. The two axes were each positioned around 0 with ±50 µm displacement. Figure 8 visualises the results for the X- and Y-axes.

The measurement was carried out under the conditions of positioning accuracy measurement of machine tools according to VDI3441 and ISO 230. A measuring point was approached at least five times from positive and negative directions and the measurement results were subsequently evaluated.

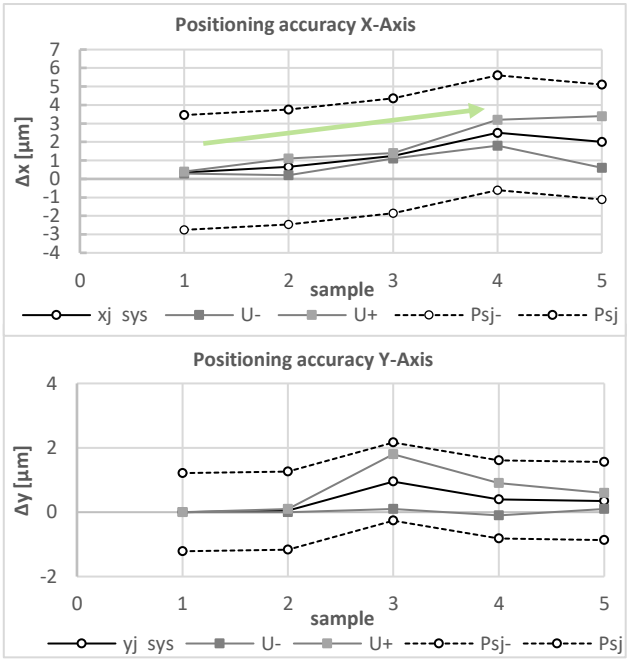

Figure 8. Positioning accuracy according to VDI3441 and ISO230

As the number of trials increases, it can be seen that a significant drift forms on the X-axis. This is due to the noise behaviour of a sensor on the X-axis, which could not be reduced even after reconfiguring the sensor and sensor controller setup several times. This noise led to the formation of a drift through the control concept, which still needs to be minimised in further optimisations. Due to this control drift, the X-axis reached a position deviation P_{ax} of 2.1 µm, whereas the Y-axis showed P_{ay} of 0.95 µm. However, the position uncertainty is still taken into account via the standard deviation of the measured values. In this statistical consideration, the drift in the X-axis leads to a large position uncertainty P_x of 8.3 µm, while in the Y-axis P_y is only 2.1 µm. This also results from the small reversal margins of the Y-axis. Further measurements also showed that due to the manufacturing tolerances, the mechanisms resulted in higher parasitic movements, which must be eliminated by calibration.

4.2. Calibration of mechatronic fixture vs. OCT

For calibration, the coordinate systems of the OCT image and the two-axis mechatronic fixture were mathematically linked via a 2-by-2 transfer matrix B. This matrix connects the measured displacement of the OCT sensor with the displacement to be compensated by the actuators in the mechatronic fixture. It is determined indirectly, by its inverse matrix A, as shown in equations 1 and 2.

$$\begin{pmatrix} x \\ y \end{pmatrix}_{OCT} = A \cdot \begin{pmatrix} x \\ y \end{pmatrix}_{actuator} = \begin{pmatrix} a_{11} & a_{12} \\ a_{21} & a_{22} \end{pmatrix} \cdot \begin{pmatrix} x \\ y \end{pmatrix}_{actuator} \quad (1)$$

$$\begin{pmatrix} x \\ y \end{pmatrix}_{actuator} = A^{-1} \cdot \begin{pmatrix} x \\ y \end{pmatrix}_{OCT} = B \cdot \begin{pmatrix} x \\ y \end{pmatrix}_{OCT} \quad (2)$$

To evaluate the matrix elements, single axis movements of the mechatronic device were performed and compared with the displacement calculated from the OCT image with respect to a previously determined reference position. Based on these measurements, the transfer matrix was calculated. The inverse transfer matrix $A^{-1} = B$ can then be used to calculate the required adjustments for a displacement detected by the OCT sensor.

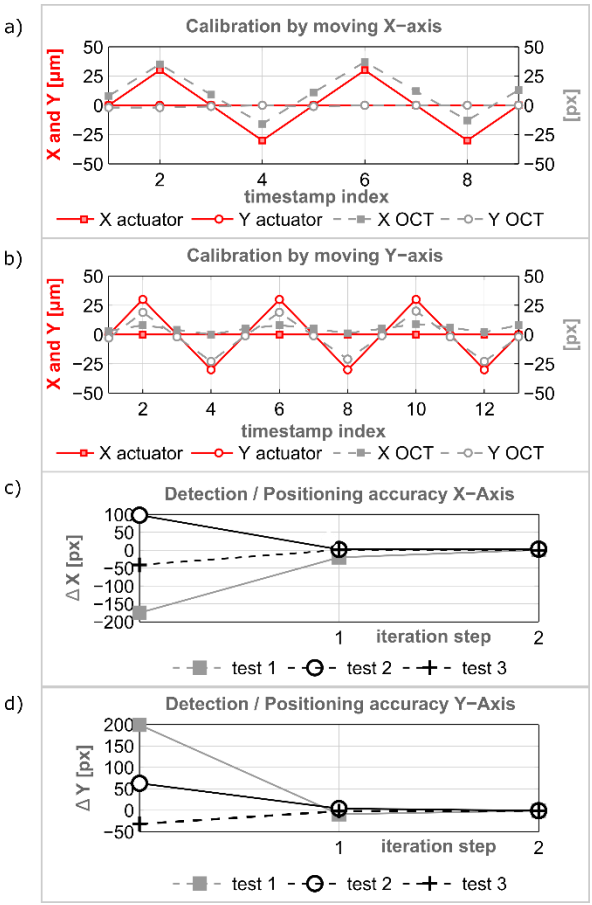

Figure 9. Calibration of transfer matrix: positions of the actuator (red), distances detected by OCT (blue). (a) Actuator movement in x-direction. (b) Actuator movement in y-direction. (c) Two step displacement compensation for x-axis. (d) Two step displacement compensation for y-axis.

Figure 9 a) and b) show the actuator-induced displacements in µm and the calculated displacements in pixels for the x- and y-axis. For the x-axis measurement, the data clearly shows the drift (as mentioned in section 4.1) of the piezo actuators. The final elements of the transfer matrix are given in equation 3. The diagonal elements of the transfer matrix give the pixel size within the scanned area: 1.18 µm/px for x- and 1.39 µm/px for y-direction. The non-zero value for a_{12} shows that there is a parasitic movement in x while moving the actuator in y-direction.

$$B = A^{-1} = \begin{pmatrix} 1.18 & 0.21 \\ 0 & 1.39 \end{pmatrix} \quad (3)$$

4.3. Pre-injection OCT-measurements

After the calibration process multiple test measurements were performed to gather information about the overall behaviour of the combined setup. A two step displacement correction test was performed to prove that the remaining displacement is small enough to comply with the FOT-specifications. Therefore, different displacements were artificially induced, then detected and finally returned to the mechatronic fixture for compensation. The remaining displacement was again measured and compensated. As can be seen in figure 9 c) and d), after the first compensation step the displacement has already been compensated to an accuracy of below 5 pixels and after the second step the remaining displacement was below 1 pixel. This shows that the method is capable of performing the displacement compensation with sufficient precision.

5. Conclusion

This paper presents an innovative application of optical coherence tomography for performing in-mould measurements. It was shown that the OCT data can be used to extract the displacement of the sample and the mould and that these displacement values can be used as an input for a displacement correction device. The remaining displacement is small enough to meet the requirements of the final product.

However, the acquired OCT data includes much more information that can be used for process and quality control. Apart from two lateral directions also the vertical surface position can be detected and analyzed with regard to flatness and tilting. In addition to pre-injection measurements also post-injection measurements are possible. These would provide information about the success of the injection moulding process and the part quality, including material inhomogeneities and damage of the bonding wires due to the injection process.

Although the described trials were successful, a few steps still have to be made in the future. First, the viewport for the OCT probe head was a flat sapphire window. For real in-mould measurements this viewport needs to have the negative shape of the lens. So far such a viewport has not yet been available. Second, before the injection moulding starts, the mould has to be closed. It is crucial that closing the mould does not cause additional displacement and the original displacement compensation is in vain. Finally, the whole compensation mechanism has yet to be built into an injection moulding machine to investigate process stability regarding applied pressure, temperature and closing forces.

Acknowledgements

This work has received funding from the European Union's Horizon 2020 research and innovation programme under grant agreement no. 820661.

References

[1] F. Fang, N. Zhang, X. Zhang, „Precision injection molding of freeform optics", *Advanced Optical Technologies*, **5**, pp. 303-324, August 2016.

[2] H. Rentzsch, S. Perz, M. Schwarze, „Mould-integrated mechatronic fixture for error compensation in injection overmoulding of optoelectronic devices", *euspen conference*, June 2020

[3] T. Ageyeva, S. Horvath, J. G. Kovacs, "In-Mold Sensors for Injection Molding: On the Way to Industry 4.0", *mpdi sensors*, August 2019

[4] D. Thomas, G. Duguid, "Optical coherence tomography – a review of the principles and contemporary uses in retinal investigation", Eye **18**, 561-570 (2004)

[5] Olsen J, Themstrup L, Jemec GB. Optical coherence tomography in dermatology. G Ital Dermatol Venereol. 2015 Oct;150(5):603-15. Epub 2015 Jul 1. PMID: 26129683.

[6] A. Nemeth, G. Hannesschläger, E. Leiss- Holzinger, K. Wiesauer, M. Leitner (March 6th 2013), "Optical Coherence Tomography – Applications in Non- Destructive Testing and Evaluation", Optical Coherence Tomography, Masanori Kawasaki, IntechOpen.

[7] M. Brezinski, "Optical coherence Tomography: principles and applications", pp. 130-134, Elsevier, 2006.